Journal of Environmental Management 392 (2025) 126652

Contents lists available at ScienceDirect

Journal of Environmental Management

journal homepage: www.elsevier.com/locate/jenvman

Research article

Control strategy to improve sustainable flux for a high-solid AnMBR in co-digesting food waste and sewage sludge

Hui Cheng [a], Kaiyi Gu [a], Yemei Li [b], Guangze Guo [c], Chang-Tang Chang [d], Wenshan Guo [e], Yu-You Li [b,d,*]

[a] School of Environmental and Chemical Engineering, Shanghai University, 333 Nanchen Road, Shanghai, 200444, China
[b] Department of Civil and Environmental Engineering, Graduate School of Engineering, Tohoku University, 6-6-06 Aoba, Aramaki-Aza, Sendai, Miyagi, 980-8579, Japan
[c] Department of Frontier Sciences for Advanced Environment, Graduate School of Environmental Studies, Tohoku University, 6-6-20 Aoba, Aramaki-Aza, Sendai, Miyagi, 980-8579, Japan
[d] Department of Environmental Engineering, National Ilan University, Yilan City, Taiwan
[e] Centre for Technology in Water and Wastewater, School of Civil and Environmental Engineering, University of Technology Sydney, Sydney, NSW, 2007, Australia

ARTICLE INFO

Keywords:
High-solid AnMBR
Anaerobic co-digestion
Control strategy of membrane filtration
Sustainable flux
Filtration-to-relaxation ratio

ABSTRACT

This study extends the previous research focused on enhancing the sustainable flux of a high-solid anaerobic membrane bioreactor (AnMBR) for the food waste (FW) and sewage sludge (SeS) co-digestion. A control strategy was implemented by adjusting instantaneous flux and filtration-to-relaxation (F/R) ratio under different total solid (TS) concentrations. The maximum sustainable fluxes of 8.7 ± 0.1, 13.3 ± 0.2, 20.3 ± 0.2, and 20.3 ± 0.6 LMH were achieved at the TS concentrations of 30, 25, 20, and 15 g/L, respectively, with corresponding optimal F/R ratios of 3:1, 5:1, 9:1, and 9:1, respectively. These sustainable fluxes were significantly improved, 4.24, 3.33, 2.18, and 2.01 times of those observed in the mono FW digestion at the same TS concentrations. Furthermore, a mathematical simulation in the form of an exponential function was developed to forecast the optimal sustainable flux at other TS levels. The improved sustainable flux of FW and SeS co-digestion than mono FW digestion might due to (1) the lower apparent viscosity, (2) the larger particle size, and (3) the synergistic effect existed in this co-digestion system. Based on the control strategy of membrane filtration, a TS concentration of 20 g/L is recommended for the AnMBR in the anaerobic co-digestion of FW and SeS. This research provides a valuable guidance for optimizing working mode of high-solid AnMBRs.

1. Introduction

The technology of anaerobic membrane bioreactor (AnMBR) has been developed for more than 40 years (Osman and Hodaifa, 2023). In the past decade, the global research interest in AnMBR has shot up due to the significant advantages (Parihar et al., 2023), including (1) independent regulation of hydraulic retention time and sludge retention time (Guo et al., 2024), (2) high biogas yield (Lei et al., 2024) and more efficient capture of organic carbon to methane (Kong et al., 2022; Wu et al., 2023), and (3) excellent effluent quality (Li et al., 2024). The industrial application of AnMBRs has also expanded from early industrial wastewater treatment, sewage treatment to organic solid waste treatment (Aslam et al., 2022; Hu et al., 2022; Zhang et al., 2024b). As for industrial wastewater treatment, AnMBR has exhibited stable treatment capability even for high salinity wastewater (Wang et al., 2023) and wastewater with refractory organics (Kong et al., 2023). In terms of sewage treatment, AnMBR is an emerging technology, offering advantages such as low energy consumption and carbon footprint, decreased greenhouse gas emission and sludge production, and high bioenergy recovery, compared to aerobic wastewater treatment processes (Min et al., 2024). Recently, AnMBR coupling with anaerobic ammonia oxidation processes has been applied to treat real sewage, and high organic carbon capture to methane, simultaneous nitrogen removal and phosphorus recovery were achieved (Guo et al., 2022b; Wu et al., 2021). With regard to organic solid waste treatment, AnMBR can efficiently convert organics into methane and achieve a high bioenergy recovery (Cheng et al., 2024; Le et al., 2022). Cheng et al. (2021) utilized a high-solid AnMBR for the treatment of food waste (FW) and sewage

* Corresponding author. Department of Civil and Environmental Engineering, Graduate School of Engineering, Tohoku University, 6-6-06 Aoba, Aramaki-Aza, Sendai, Miyagi, 980-8579, Japan.
E-mail addresses: chenghui@shu.edu.cn (H. Cheng), gyokuyu.ri.a5@tohoku.ac.jp (Y.-Y. Li).

https://doi.org/10.1016/j.jenvman.2025.126652
Received 7 April 2025; Received in revised form 2 July 2025; Accepted 16 July 2025
Available online 2 August 2025
0301-4797/© 2025 The Authors. Published by Elsevier Ltd. This is an open access article under the CC BY-NC license (http://creativecommons.org/licenses/by-nc/4.0/).

sludge (SeS), and a high COD conversion efficiency of >90 % and a high energy recovery of 28.35 kJ/g-VS were achieved.

However, one of the main challenges faced by AnMBRs in practical applications is membrane fouling or flux decline (Lei et al., 2021b; Min et al., 2024; Zhou et al., 2019). Membrane fouling is the deposition, accumulation, or obstruction of foulants on the membrane surface and/or in its pores, resulting in a flux decline and the increase of filtration resistance and transmembrane pressure (TMP) (Fan et al., 2024). Particles with size smaller than the membrane pores can enter the membrane pores and retain inside the filtration channels, causing a pore blockage. Particles with size similar or larger than the membrane pores are apt to gather on the membrane surface, leading to the formation of a cake layer. Colloid substances, extracellular polymeric substances, and soluble microbial products have a tendency of adsorption and aggregation on the membrane surface, forming a gel layer. Therefore, mitigating membrane fouling has become a top priority. Various strategies have been developed to control membrane fouling, including (1) adding adsorbents (Jiao et al., 2025; Lei et al., 2021a), bio-carriers (Jiang et al., 2022), and flocculants (Zhang et al., 2017), (2) modifying the membrane (Hung et al., 2024), (3) adopting ultrasonic technology (Naji et al., 2021), (4) integrating with an electrochemical system (Deng et al., 2023), (5) implementing quorum quenching techniques (Kim et al., 2024), and (6) optimizing biogas sparging strategy (Olubukola et al., 2022) and regulating agitation speed (Zhang et al., 2024a). Despite the effectiveness of these fouling control methods, their industrial application often faces several limitations, including high chemical and energy consumption, complex operation, and elevated operating costs (Maaz et al., 2019). In recent years, filtration mode optimization has garnered increasing attention from both academia and industry as a promising approach to mitigate membrane fouling and enhance operational longevity (Cheng et al., 2020b; Guo et al., 2022; Hu et al., 2021; Jiang et al., 2023). This strategy eliminates the need for chemical additives and focuses on adjusting operational parameters — specifically, the instantaneous flux and the filtration-to-relaxation (F/R) ratio — thereby offering a simplified and cost-effective solution. Cheng et al. (2020b) reported that, through filtration mode optimization, the sustainable flux in an AnMBR treating FW increased by 29 %, 35 %, 52 %, and 21 % at MLTS concentrations of 10, 15, 20, and 25 g/L, respectively.

As for membrane operation, there are three important definitions on flux: critical flux, threshold flux, and sustainable flux. Critical flux is defined as the flux below which no time-dependent flux decline occurs, whereas fouling appears above it (Field et al., 1995; Liu et al., 2023). Critical flux is generally too low which is not applicable for large-scale processing in industrial application. Threshold flux denotes a particular flux level. Once the actual flux surpasses this threshold, the rate of membrane fouling will accelerate significantly. By contrast, sustainable flux is usually higher than critical flux and lower than threshold flux, and when the operating flux is at or lower than this value, the membrane operation can maintain a relatively sluggish fouling rate, which renders it suitable and practical for reality applications. Membrane operated at sustainable flux can achieve acceptable and moderate membrane fouling and a balance between capital expenditure and operating costs (Field and Pearce, 2011). Thus, how to enhance sustainable flux has become an urgent problem.

With the acceleration of urbanization and the improvement of citizens' living standards, FW production has increased by a big margin. Nineteen percent of food available to consumers is wasted according to a survey by Food and Agriculture Organization of the United Nations (FAO, 2022). By 2025, the global amount of FW is estimated to reach 2.5×10^9 tons (Zhang et al., 2023). SeS, the most important byproduct of municipal wastewater treatment plant, is an another important composition of urban organic solid waste. The dry SeS production is projected to reach 68 million tons worldwide by 2050 (Molaey et al., 2024). A high-solid AnMBR has emerged as a promising treatment for anaerobic co-digestion of FW and SeS (Hu et al., 2022; Li et al., 2023). Given the high content of total solids (TS) in FW and SeS, a high-solid AnMBR is a judicious choice. However, further research is required to control membrane fouling and maintain a high sustainable flux at such a high TS concentration. This will prove to be an important step in the treatment of FW and SeS by using AnMBRs.

This research presents several innovative contributions to the field of high-solid AnMBRs for the anaerobic co-digestion of FW and SeS. Firstly, it pioneers a control strategy of membrane filtration by optimizing the filtration mode for this co-digestion system at varying TS concentrations. This novel approach by precisely adjusting instantaneous flux and F/R ratio leads to a remarkable enhancement in sustainable flux. Secondly, a mathematical simulation in the form of an exponential function is developed to forecast the sustainable flux at different TS levels, filling a gap in membrane performance prediction. Finally, the research reveals the mechanism behind the enhanced sustainable flux in the FW and SeS co-digestion compared to the mono FW digestion, which offers in-depth theoretical insights for process optimization.

2. Material and methods

2.1. Inoculum and substrate

The seed sludge originated from a mesophilic FW anaerobic digestion tank. The characteristics of the substrate used in this research are detailed in Table 1, and the co-substrate was FW and SeS, with a TS concentration of 44.4 ± 1.3 g/L and a COD concentration of 58.3 ± 7.1 g/L. The FW preparation followed the formula outlined in a previous literature (Cheng et al., 2018). SeS was a mixture of primary sludge and secondary sludge, and the mass ratio was 45 %:55 %. The mixing ratio of FW:SeS was 50 %:50 % (based on TS).

2.2. Reactor configuration

The AnMBR system consisted of a continuous stirred tank reactor and a membrane unit, with a total effective operating volume of 15 L. The membrane unit was equipped with a hollow fiber membrane (Sumitomo Electric Industries Ltd.). The total membrane area is 0.1 m^2 and the pore size is between 0.1 and 0.2 μm. The operating temperature of the AnMBR was kept at 35 °C, with an allowable fluctuation of ±2 °C. The biogas sparging rate was maintained at 5 L/min to control membrane fouling. The operation status of the membrane was monitored in real-time by an online Keyence TMP analyzer and a pressure sensor. Further details of the AnMBR system are accessible in our previous publication (Cheng et al., 2021).

2.3. The adjustment of TS concentrations and the filtration mode optimization

Taking the TS concentrations as the foundation, the experiment was carried out in four successive stages, with a concentration of 30 g-TS/L in Stage I, 25 g-TS/L in Stage II, 20 g-TS/L in Stage III, and 15 g-TS/L in Stage IV. The average concentrations of TS, VS, SS, and VSS in the four

Table 1
Characteristics of the substrate.

Parameter	Unit	Value
TS	g/L	44.4 ± 1.3
VS	g/L	40.4 ± 0.3
T-COD	g/L	58.3 ± 7.1
S-COD	g/L	17.5 ± 2.3
T-carbohydrate	g/L	15.9 ± 0.4
S-carbohydrate	g/L	5.5 ± 4.3
T-protein	g/L	17.0 ± 3.0
S-protein	g/L	1.5 ± 0.1
NH_4^+-N	mg/L	325 ± 19
C/N ratio	–	14.0 ± 0.1

TS: total solids; VS: volatile solids.

stages are shown in Table 2. The operation conditions of the AnMBR and the average performance achieved during the stable period are displayed in Table 3. TS concentrations were adjusted by discharging sludge and adding tap water to maintain a constant volume of mixed liquor in the AnMBR, and the volume of discharged sludge was calculated by the following formula.

$$\frac{C_{i+1} \times V_{reactor}}{C_i} = V_{reactor} - V_{discharged}$$

Where C_i is the TS concentration in Stage i, C_{i+1} is the TS concentration in Stage i+1, $V_{reactor}$ is the reactor volume (15 L), $V_{discharged}$ is the volume of discharged sludge.

The optimization experiment of filtration mode was conducted as outlined in Table 4. Taking TS = 30 g/L as an example, the operation process was stable under the mode of 3-min filtration and 1-min relaxation, but when the filtration time was extended to 4 min (F/R = 4:1), instability occurred, as manifested by a sharp rise in TMP. Then the F/R ratio was reset to 3:1 (the optimal F/R ratio), while the instantaneous flux was increased from 12 to 15 LMH, aiming to determine the maximum sustainable flux.

The instantaneous flux ($J_{inst.}$), average flux ($J_{avg.}$), and resistance (R_T) were calculated by the formulas in **Supplementary materials**, and other analysis projects and methods have been explicitly recorded in a previous literature (Cheng et al., 2020b).

2.4. Mathematical simulation

The DoseResp model in the drawing software Origin was used for mathematical simulation, and an exponential function related to maximum sustainable flux and TS concentration was obtained.

3. Results and discussion

3.1. The long-term performance of the high-solid AnMBR

In the long-term continuous experiment, the organic loading rate (OLR) was 3.89 ± 0.47 g-COD/L/d, and the hydraulic retention time was 15 days. The entire experiment was divided into four stages, and the average TS concentration was 30 g/L (Stage I), 25 g/L (Stage II), 20 g/L (Stage III), and 15 g/L (Stage IV), as mentioned in Section 2.3.

The performance of the high-solid AnMBR in the FW and SeS co-digestion system is shown in Table 3 and Fig. 1. The biogas production rate and methane yield was 1.68 ± 0.31 L/L-reactor/d and 0.25 ± 0.03 L-CH_4/g-$COD_{re.}$, respectively. The methane content in the biogas was 60.20 ± 1.00 %. The ammonia concentration (1343 ± 353 mg/L), alkalinity (3918 ± 220 mg-$CaCO_3$/L), total volatile fatty acids (VFAs) concentration (12 ± 1.2 mg-CH_3COOH/L), and pH value (7.3 ± 0.1) in the AnMBR all maintained within the favorable ranges for anaerobic digestion. Moreover, an outstanding treatment efficiency was achieved, as evidenced by a low COD concentration in the effluent of 390 ± 60 mg/L and a COD removal efficiency of 99.30 ± 0.17 %. Carbohydrates and proteins, as the main contributors to COD, also had low concentrations in the effluent, which were 30 ± 3 and 131 ± 37 mg/L, respectively.

Table 2
Average TS, VS, SS and VSS concentrations of the four stages.

	Stage I	Stage II	Stage III	Stage IV
TS (g/L)	29.83 ± 1.72	25.63 ± 1.36	20.92 ± 1.04	15.84 ± 1.10
VS (g/L)	23.61 ± 1.00	21.19 ± 1.28	17.99 ± 1.10	12.69 ± 1.21
SS (g/L)	27.63 ± 2.42	20.60 ± 1.91	17.47 ± 0.81	12.16 ± 0.93
VSS (g/L)	22.55 ± 1.61	18.42 ± 1.23	15.93 ± 0.52	10.32 ± 0.82

TS: total solids; VS: volatile solids; SS: suspended solids; VSS: volatile suspended solids.

Table 3
AnMBR operation conditions and the average performance obtained during the stable period.

Biogas production	OLR (g-COD/L/d)	3.89 ± 0.47
	HRT (d)	15
	L/L-reactor/d	1.68 ± 0.31
	L/g-TS_{in}	0.56 ± 0.04
	L-CH_4/g-COD_{re}	0.25 ± 0.03
	Biogas composition	
	CH_4 (%)	60.20 ± 1.00
	CO_2 (%)	38.40 ± 0.98
	H_2S (ppm)	608 ± 188
Reactor stability	pH	7.3 ± 0.1
	Alkalinity (mg-$CaCO_3$/L)	3918 ± 220
	VFA (mg-HAC/L)	12 ± 1.2
	NH_4^+-N (mg /L)	1343 ± 353
Effluent quality	COD (mg/L)	390 ± 60
	Carbohydrate (mg/L)	30 ± 3
	Protein (mg/L)	131 ± 37
Organic removal efficiency	COD (%)	99.30 ± 0.17
	Carbohydrate (%)	99.80 ± 0.11
	Protein (%)	99.20 ± 0.65

Table 4
Process of the filtration mode optimization: different F/R ratios and instantaneous fluxes applied at TS concentrations of 30, 25, 20, and 15 g/L.

No.	TS (g/L)	F/R ratio (min:min)	$J_{inst.}$ (LMH)	$J_{avg.}$ (LMH)
1	30	3:3	12	5.9
2		3:2	12	7.0
3		3:1	12	8.7
4		4:1	12	[a]
5		3:1	15	[a]
6	25	3:3	12	6.2
7		3:2	12	7.4
8		3:1	12	9.1
9		4:1	12	9.5
10		5:1	12	9.7
11		6:1	12	[a]
12		5:1	15	13.3
13		5:1	18	[a]
14	20	3:3	18	8.8
15		3:2	18	10.8
16		3:1	18	13.1
17		4:1	18	14.9
18		5:1	18	15.0
19		6:1	18	15.4
20		7:1	18	15.7
21		8:1	18	16.4
22		9:1	18	16.3
23		9:1	21	18.0
24		9:1	24	20.3
25		9:1	27	[a]
26	15	3:3	24	12.5
27		3:2	24	14.8
28		3:1	24	18.5
29		4:1	24	19.8
30		5:1	24	19.9
31		6:1	24	20.7
32		7:1	24	20.7
33		8:1	24	20.3
34		9:1	24	20.3
35		9:1	27	[a]

[a] Unsustainable operation, the flux decreased or TMP increased with time.

3.2. Filtration mode optimization

In the continuous experiment on the anaerobic co-digestion of FW and SeS, the control strategy of membrane filtration was explored by optimizing the filtration mode at varying TS concentrations to enhance the sustainable flux. A comprehensive evaluation of the long-term

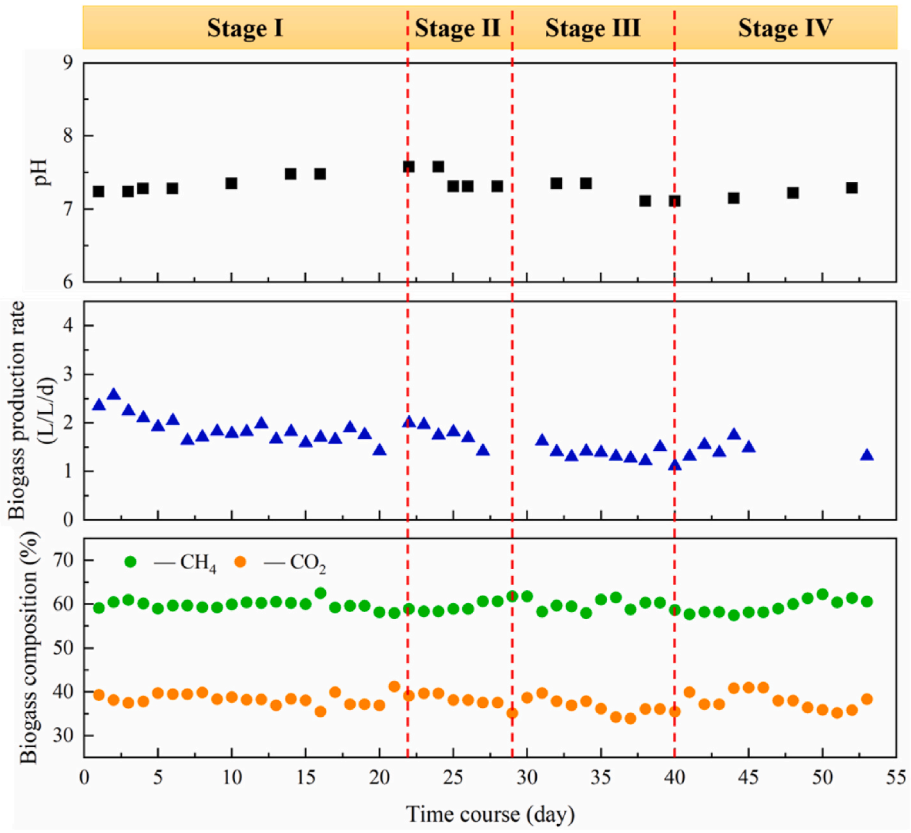

Fig. 1. The changes in pH value, biogas production rate and biogas composition over time in the FW and SeS co-digestion.

membrane performance was presented in the previous literature (Cheng et al., 2020a), and the filtration mode experiment in this study was conducted during the phase where the FW:SeS ratio was 50 %:50 %. As shown in Table 4, six instantaneous fluxes and nine F/R ratios were applied. Filtration modes were trialed at the mixed liquor concentrations of 30, 25, 20, and 15 g-TS/L, with the evaluation of five, eight, twelve, and ten modes, respectively. The average flux and resistance under each filtration mode were calculated. As presented in Figs. 2 and 3, owing to the large amount of experimental data for filtration mode optimization, only three representative curves for each TS concentration were given: (1) a low sustainable flux operation (LSFO), (2) the maximum sustainable flux operation (MSFO), and (3) an unsustainable flux operation (USFO). Besides, based on the critical flux and threshold flux in the mono FW digestion obtained from the previous study (Cheng et al., 2020b) at the TS concentrations of 10, 15, 20, and 25 g/L, the corresponding values for TS = 30 g/L were predicted to be 1.25 and 2.4 LMH, respectively, as shown in Table 5.

The optimization of filtration mode started with a TS concentration at 30 g/L (Stage I). As depicted in Figs. 2 and 3 (a)-top, the TMP kept steady at 2.93 ± 0.10 kPa when the F/R ratio was 3:3 and the instantaneous flux was 12 LMH, the average flux remained at 5.9 ± 0.1 LMH, and the resistance was (2.59 ± 0.04) × 10^{11}/m. Then the relaxation time was shortened to 2 min and 1 min (F/R = 3:2 and 3:1) at the same instantaneous flux of 12 LMH. It can be observed from Figs. 2 and 3 (a)-middle that the average flux rose to 8.7 ± 0.1 LMH at the F/R ratio of 3:1, significantly surpassing the threshold flux of the mono FW digestion at 2.4 LMH in Table .5, and the TMP remained at 5.54 ± 0.36 kPa, the resistance stayed at (3.29 ± 0.22) × 10^{11}/m. During the membrane operation in this filtration mode, no noticeable flux decline or TMP increase was observed. The stable TMP, average flux, and resistance implied the sustainability of the membrane operation at this filtration mode. To further enhance sustainable flux, the filtration time was increased to 4 min at the same instantaneous flux and relaxation time ($J_{inst.}$ = 12 LMH, F/R ratio = 4:1). As it is shown clearly in Figs. 2 and 3 (a)-bottom, both the TMP and resistance significantly increased from 4.27 to 6.89 kPa and from 2.28 × 10^{11} to 4.08 × 10^{11}/m, indicating that the membrane was unable to sustainably operate under this filtration mode. These optimization findings suggested that the optimal filtration mode for the concentration of 30 g-TS/L was as follow: the instantaneous flux = 12 LMH and the F/R ratio = 3:1, and the maximum sustainable flux achieved was 8.9 ± 0.1 LMH.

Then TS concentration was reduced to 25 g/L (Stage II), and the filtration mode optimization experiment began with the instantaneous flux at 12 LMH and the F/R ratio at 3:3. The membrane could still operate sustainably with the increase of the F/R ratio from 3:3 to 5:1 when the instantaneous flux was the same as 12 LMH. For instance, at the F/R ratio of 3:3 and the instantaneous flux of 12 LMH, the average flux attained a value of 6.2 ± 0.1 LMH, the TMP remained steady at 2.86 ± 0.04 kPa, and the resistance kept constant at (2.39 ± 0.07) × 10^{11}/m, as illustrated in Figs. 2 and 3 (b)-top. When F/R ratio was further raised from 5:1 to 6:1 and the instantaneous flux was kept at 12 LMH, as shown in Table 4, an unsustainable operation of the membrane occurred. Then the F/R ratio was return to 5:1 and the instantaneous flux was raised to 15 LMH, the average flux climbed to 13.3 ± 0.2 LMH, and the TMP and the resistance exhibited stability at 7.04 ± 0.17 kPa and (2.73 ± 0.09) × 10^{11}/m (Figs. 2 and 3 (b)-middle), indicating the sustainable filtration mode. Aimed at further boosting the average flux, while maintaining the same F/R ratio of 5:1, the instantaneous flux rose to 18 LMH. However, as is evidently depicted in Figs. 2 and 3 (b)-bottom, the TMP increased from 10.72 to 11.91 kPa, in the company of the average flux sharply dropping from 14.5 to 12.5 LMH, demonstrating that the membrane operation was unstable. The resistance fluctuations, TMP, and average flux reflected that the optimal filtration mode for the concentration of 25 g-TS/L was achieved at the instantaneous flux of 15 LMH and the F/R ratio of 5:1. Under these conditions, the maximum sustainable flux was determined to be 13.3 ± 0.2 LMH.

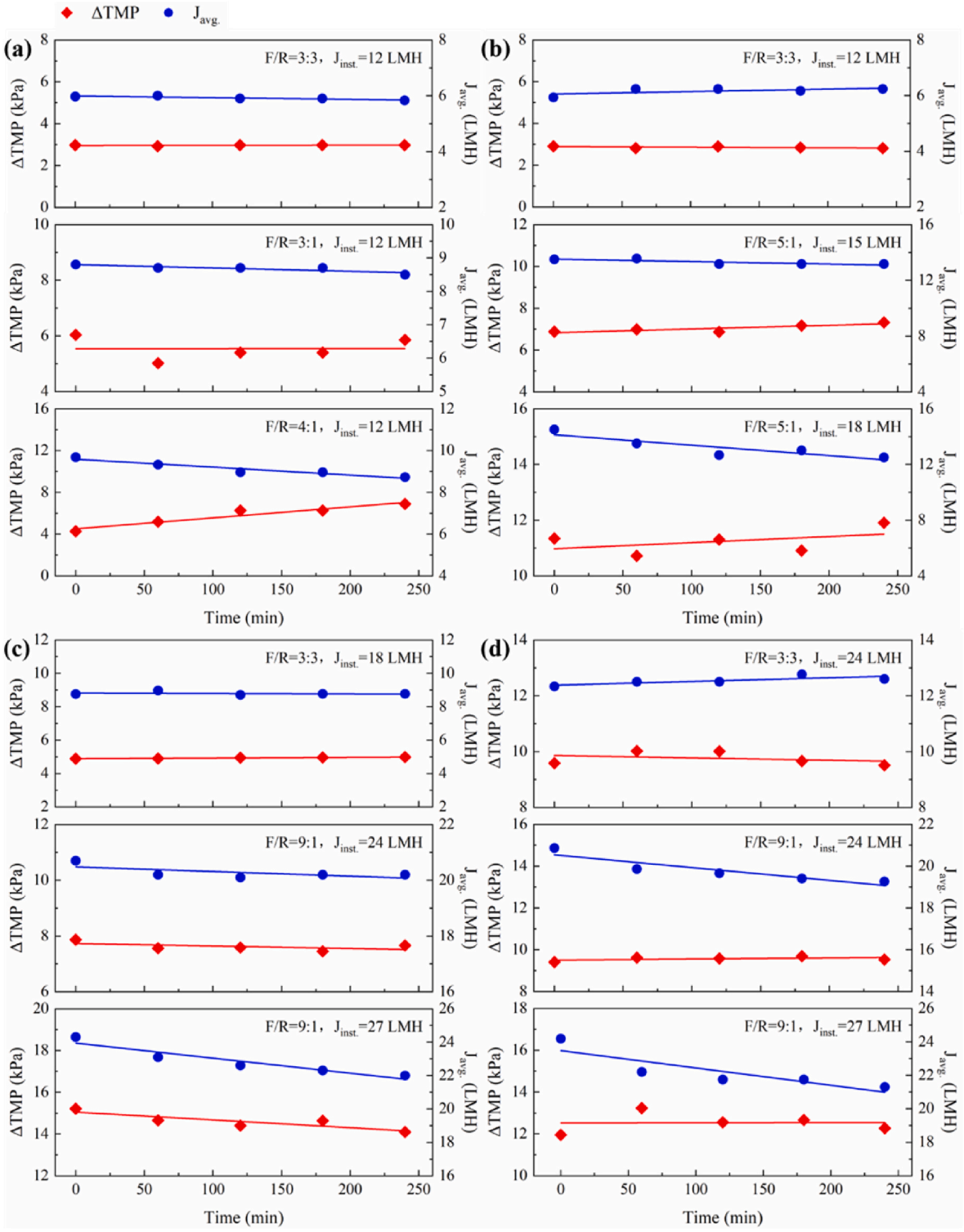

Fig. 2. TMP and average flux as a function of time at different TS concentrations in the FW and SeS co-digestion: (a) TS = 30 g/L; (b) TS = 25 g/L; (c) TS = 20 g/L; (d) TS = 15 g/L. There are three subfigures in Fig. 2 (a), (b), (c), and (d), the top, middle, and bottom subfigure showing TMP and average flux changes under a low sustainable flux operation (LSFO), the maximum sustainable flux operation (MSFO), and the unsustainable flux operation (USFO), respectively.
Note: A series of filtration mode optimizations were performed at each TS concentration according to Table 4, but only three representative curves are presented in this figure.

The optimization experiment of filtration mode was also performed at the concentrations of 20 and 15 g-TS/L. When the concentration of mixed liquor was 20 g-TS/L (Figs. 2 and 3 (c)), the optimal filtration mode was achieved at the F/R ratio of 9:1 and the instantaneous flux of 24 LMH, with the corresponding maximum sustainable flux reaching 20.3 ± 0.2 LMH. The optimal filtration mode was unchanged when further decreasing the concentration to 15 g-TS/L (Figs. 2 and 3 (d)), with the F/R ratio at 9:1 and the instantaneous flux at 24 LMH, and similar maximum sustainable flux was achieved at 20.3 ± 0.6 LMH. Although different from the previous expectation and report that the

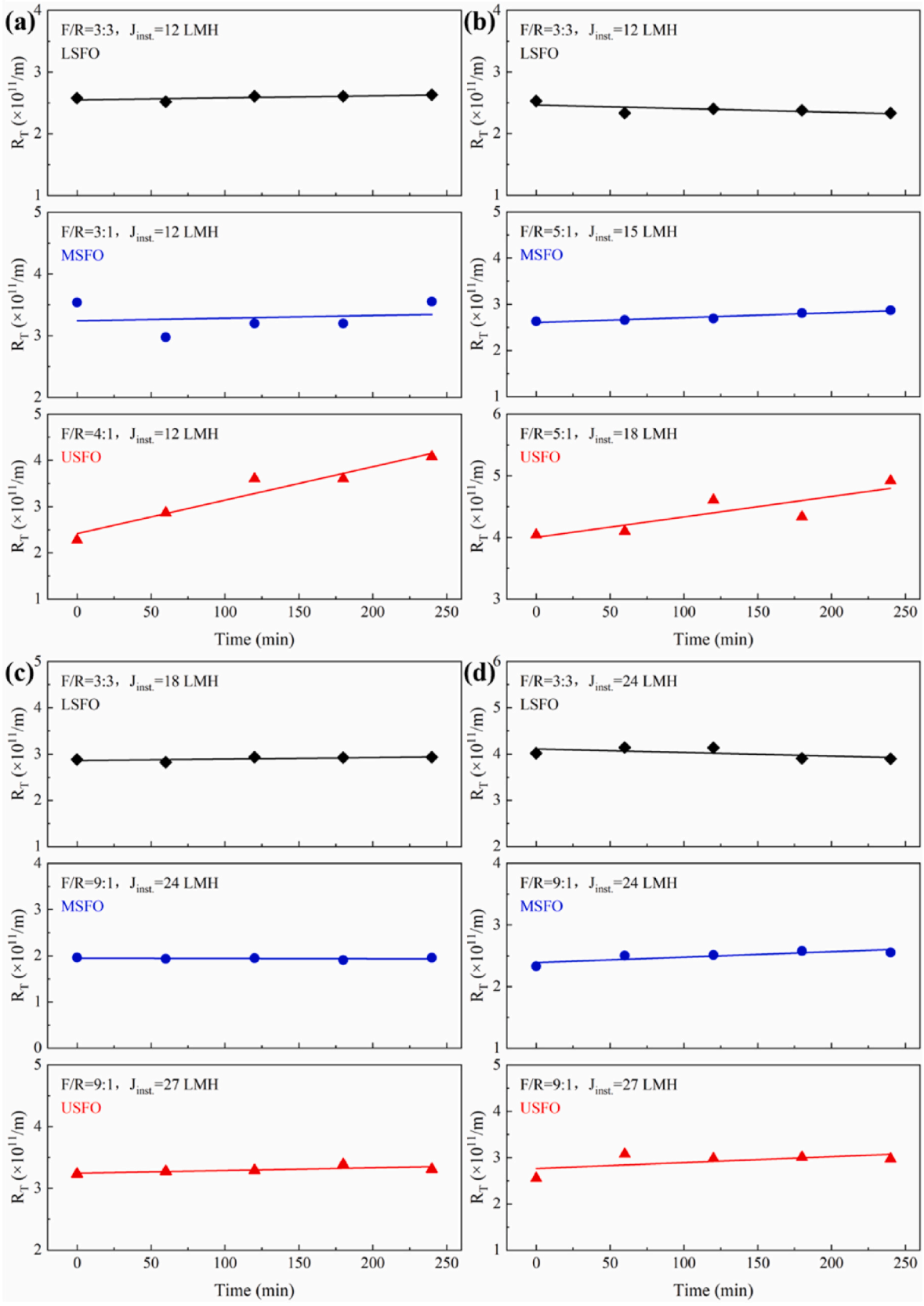

Fig. 3. Resistance as a function of time at different TS concentrations in the FW and SeS co-digestion: (a) TS = 30 g/L; (b) TS = 25 g/L; (c) TS = 20 g/L; (d) TS = 15 g/L.

Table 5
Critical fluxes and threshold fluxes at different TS concentrations in the mono FW digestion.

TS (g/L)	J_c (LMH)	J_t (LMH)
10	10.2	16.8
15	7.5	10.9
20	6.1	9.4
25	3.3	6.1
30 (Predicated)	1.25	2.4

resistance of membrane filtration increased (and the sustainable flux decreased) exponentially as the TS concentration increased (Guo et al., 2024), the findings of this research aligned with the observation of Mahmoud and Liao (2017) and Ji et al. (2021). The sustainable flux decreased as the MLTS concentration increased from 5.7 to 10.6 g/L, and until the MLTS concentration climbed to 15.0 g/L, it stabilized and remained nearly constant in the study of Mahmoud and Liao (2017). Similarly, Ji et al. (2021) found that the permeability decreased with the increase of MLSS from 8.2 to 12.2 g/L, but when the MLSS concentration rose from 14.3 to 20.2 g/L, no clear decrease emerged. According to the analysis of external forces exerted on the particles during membrane filtration period in our previous study (Cheng et al., 2020a), this stabilization of flux might due to the fact that the effect of biogas sparging (the shear force) and the transport of particles to the membrane (the permeation drag force) achieved a dynamic balance during the membrane filtration phase in the TS range of 15–20 g/L (Mahmoud and Liao, 2017). At this TS range, these opposing forces may reach equilibrium, thereby limiting further increases in particle deposition on the membrane surface and stabilizing the flux. Further studies are needed to explore the underlying mechanisms of this stabilization phenomenon.

In summary, the optimal filtration modes for the TS concentrations of 30, 25, 20, and 15 g/L were at the F/R ratio of 3:1, 5:1, 9:1, and 9:1 and the instantaneous flux of 12, 15, 24, and 24 LMH, respectively. The maximum sustainable fluxes achieved in this research were up to 8.7 ± 0.1, 13.3 ± 0.2, 20.3 ± 0.2, and 20.3 ± 0.6 LMH, much higher than the critical fluxes and threshold fluxes of the mono FW digestion (Table 5). Although the maximum sustainable flux at 20 g-TS/L is nearly equivalent to that at 15 g-TS/L, operating at 20 g-TS/L offers greater treatment capacity, which enhances the overall efficiency of the system. Compared to higher concentrations (25 and 30 g-TS/L), 20 g-TS/L results in a significantly slower rate of membrane fouling, contributing to more stable long-term operation. From an economic standpoint, the membrane service life at 20 g-TS/L is expected to be longer than at higher TS levels, reducing the frequency of membrane replacement. This translates into lower operational costs and improved system sustainability. To sum up, considering the trade-offs between flux, fouling rate, treatment capacity, and cost efficiency — along with the optimization results of the filtration mode — 20 g-TS/L is identified as the most practical and effective concentration for operation.

A mathematical simulation was performed by using the DoseResp model in the drawing software Origin and an exponential function ($y = 8.7 + \frac{11.6}{1+10^{-0.33333\times(23.28571-x)}}$, $R^2 = 0.94483$) was obtained correlating maximum sustainable flux and TS concentration, as shown in Fig. 4. The exponential function performed to interpret the experimental data has a high reliability on the basis of the high determination coefficient. This function can be utilized to forecast the maximum sustainable flux at other TS levels, which can provide a valuable guidance for optimizing working mode of high-solid AnMBRs.

3.3. Mechanism behind the enhanced sustainable flux of the FW and SeS co-digestion in contrast to the mono FW digestion

According to the regression equation obtained from the mono FW digestion system (Cheng et al., 2020b), the maximum sustainable flux was 2.05 LMH at the mixed liquor concentration of 30 g-TS/L. Similarly,

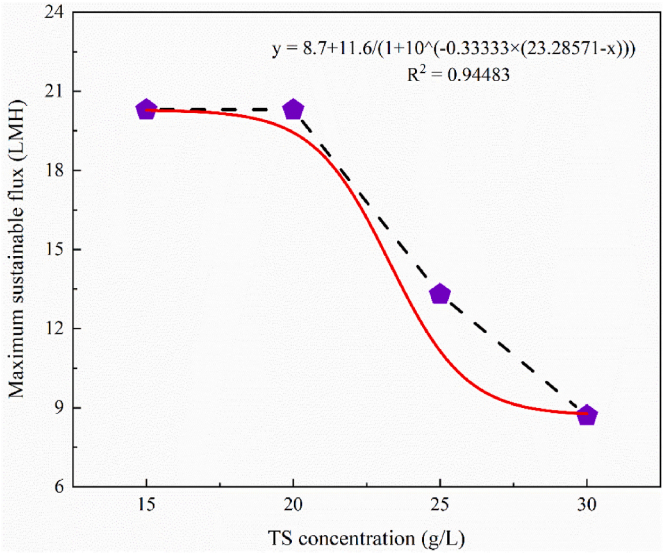

Fig. 4. The mathematical simulation between maximum sustainable flux and TS concentration in the FW and SeS co-digestion.

in the FW and SeS co-digestion system, the maximum sustainable flux at the concentration of 10 g-TS/L was 20.3 LMH. It is shown clearly in Fig. 5 (a) that the maximum sustainable fluxes of the FW and SeS co-digestion were greatly enhanced at the concentration of 30, 25, 20, 15, and 10 g-TS/L, 4.24, 3.33, 2.18, 2.01, and 1.54 times as high as those of mono FW digestion.

In contrast to the mono FW digestion, the higher maximum sustainable flux of the FW and SeS co-digestion might due to (1) the lower apparent viscosity, (2) the larger particle size, and (3) the synergistic effect existed in this co-digestion system. Cao et al. (2023) observed that the apparent viscosity of the FW and SeS co-digestate, mono SeS digestate and mono FW digestate was ranked as follows: FW and SeS co-digestate < mono SeS digestate < mono FW digestate, and the apparent viscosity was significantly positively correlated with soluble COD (SCOD) content. The SCOD concentrations of the FW and SeS co-digestion and mono FW digestion were 0.31 ± 0.16 and 0.76 ± 0.29 g/L, as depicted in Fig. 5 (b). The lower SCOD concentration in the FW and SeS co-digestion evidenced the lower viscosity and better fluidity of co-digestion. The lower apparent viscosity of the FW and SeS co-digestion reduced the adhesion of foulants inside the pore channels and/or on the membrane surface, thereby alleviating membrane fouling and helping to boost sustainable flux. This is in good agreement with the findings in this research and previous publications (Cheng et al., 2020b; Guo et al., 2022) that the sustainable fluxes of the FW and SeS co-digestion, mono SeS digestion and mono FW digestion were ranked: FW and SeS co-digestion > mono SeS digestion > mono FW digestion at the same TS concentration. For instance, the sustainable flux of the FW and SeS co-digestion was 13.3 LMH > mono SeS digestion at 9.6 LMH (Guo et al., 2022) > mono FW digestion at 4.0 LMH (Cheng et al., 2020b) when the TS concentration was 25 g/L. In addition, in our study, the viscosity of mono FW digestate (35.0 mPa s) was higher than that of mono SeS digestate (26.1 mPa s), which was consistent with the findings of Cao et al. (2023).

Particle size of the mixed liquor from the FW and SeS co-digestion system and the mono FW digestion system were also measured. In the FW and SeS co-digestion, a broad particle distribution (3–3000 μm) was observed in Fig. 5 (c), with a dominant peak from 3 to 400 μm, while a unimodal with a preponderant peak between 2 and 1000 μm was found in the mono FW digestion. Despite the differences in different peak shapes and locations, the particles in the mixed liquor of both FW and SeS co-digestion and mono FW digestion were invariably larger than the size of membrane pore (0.1 μm). This indicated that the particles were

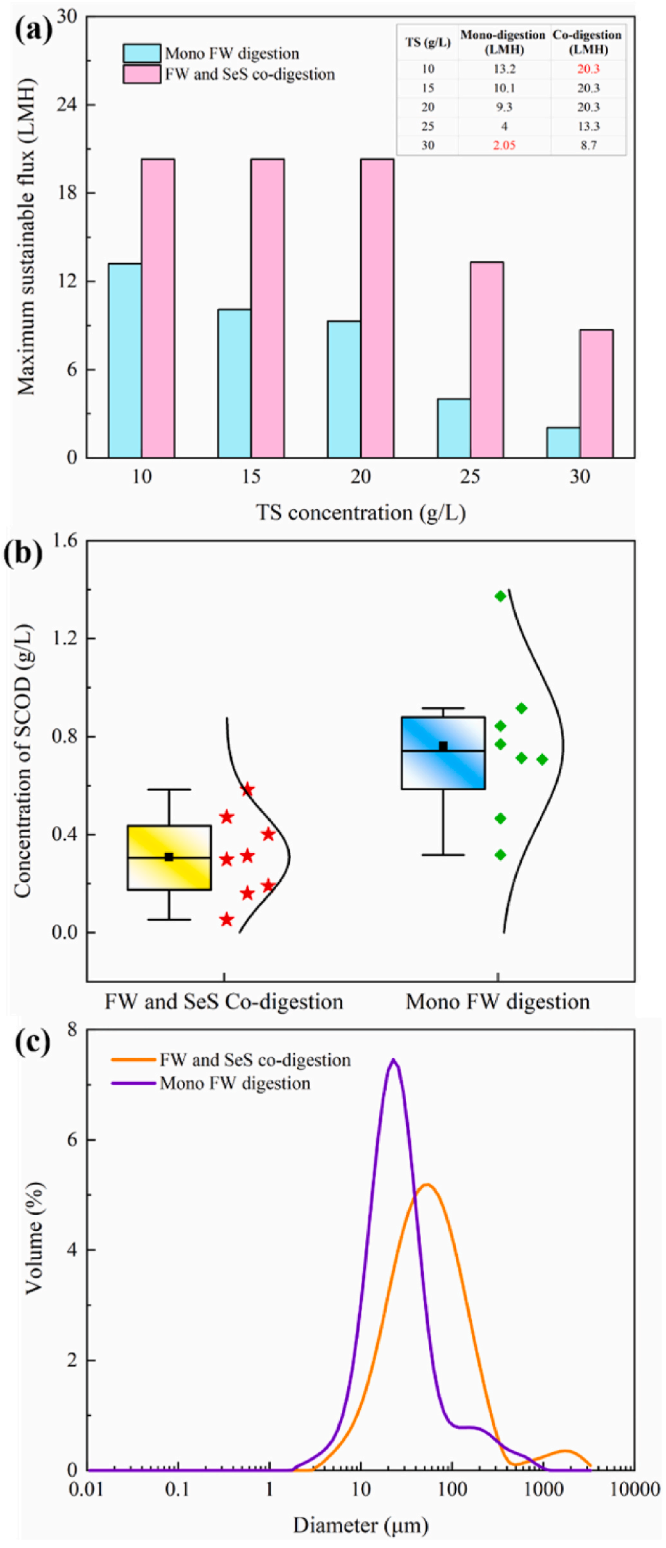

Fig. 5. Comparison between mono FW digestion and FW and SeS co-digestion: (a) maximum sustainable fluxes; (b) distribution of SCOD concentrations; (c) particle size distribution of the mixed liquor in the AnMBR.
Note: The red values are calculated from the equations in Fig. 4 (a), while the black values are the experimentally measured data.

mainly accumulated and deposited on the membrane surface, forming the cake layer. It is important to note that there were more particles with a diameter of <3 μm in the mono FW digestion than in the FW and SeS co-digestion, which might fill the interstices in the cake to make the cake layer denser. Park et al. (2006) found that, the number of particles in the cake layer increased markedly at the same feed concentration as particle size decreased, and smaller particles created a larger hydraulic resistance to permeate flow, triggering an increased fouling index. The more particles with a diameter of <3 μm in the mono FW digestion led to a severe membrane fouling and the lower sustainable flux compared to the FW and SeS co-digestion.

Furthermore, there exists a synergistic effect in the anaerobic co-digestion (Pan et al., 2019). In the FW and SeS co-digestion system, FW provides SeS with easily degradable carbon source, while SeS compensates for trace elements for FW. At the same time, the activity and degradation capacity of microorganisms (such as the strict aceto-clastic methanogens *Methanosaeta concilii*) are enhanced during anaerobic co-digestion (Li et al., 2023; Wang et al., 2021), which helps the degradation of organic matters and reduces the accumulation and deposition of suspended solids on the membrane surface and/or inside the pore channels. Anaerobic co-digestion has also been reported to improve fluidity of mixed liquor/digestate (Cao et al., 2023). These are the reasons that contribute to a low membrane fouling rate and a high sustainable flux.

3.4. Typical membrane filtration processes

Typical real-time TMP curves of the FW and SeS co-digestion under different filtration modes at the TS concentration of 30 g/L were presented in Fig. 6 (a)–(d), including (1) a sustainable process at a low flux, (2) a sustainable process at the maximum sustainable flux, (3) an unsustainable process induced by excessive instantaneous flux, and (4) an unsustainable process induced by inadequate relaxation time. Fig. 6 (a) shows the real-time TMP curve under a sustainable process at a low average flux of 6 LMH, with the F/R ratio of 3:3 and the instantaneous flux of 12 LMH. Under this filtration mode, after filtration phase, both TMP_0 and TMP_t could recover and return to their original values. The combination of the stable TMP, flux, and R_T (shown in Figs. 2 and 3 (a)-top) indicated a long-term sustainable operation. To enhance average flux, the relaxation time was reduced to 2 and 1 min. Fig. 6 (b) displays the real-time variation curve of TMP under the maximum sustainable flux operation mode with the instantaneous flux of 12 LMH and the F/R ratio of 3:1. This curve is characterized by the returnable TMP_0 and TMP_t and stable flux and R_T. Fig. 6 (c) and (d) show the unsustainable operations induced by excessive instantaneous flux and inadequate relaxation time, which exhibit a small amplitude variation of TMP_0 and a gradually increase in TMP_t.

It should be noted that this was different from the real-time TMP curves of a mixed liquor with a high apparent viscosity such as mono FW digestate (Cheng et al., 2020b). Under an unsustainable process induced by excessive instantaneous flux, the real-time TMP curve of a mixed liquor with a high apparent viscosity is characterized by an increased TMP_t, followed by an increase in TMP_0, and the increasing rate of TMP_t ($k_2 = \frac{d\ TMP_t}{d\ t}$) is higher than that of TMP_0 ($k_1 = \frac{d\ TMP_0}{d\ t}$), namely $k_2 > k_1$ (as shown in Fig. 6 (e)). TMP_0 will increase firstly under an unsustainable operation induced by inadequate relaxation time (Fig. 6 (f)), which causes the increase of TMP_t, and the slop of TMP_0 is larger than that of TMP_t ($k_1' > k_2'$). During filtration phase, the permeation drag force greatly exceeds the back transport force, and sludge flocs or particles migrate towards the membrane under the action of the permeation drag force and accumulate on its surface. At the beginning of relaxation phase, because of the relief of transmembrane suction pressure, a mixed liquor with a lower apparent viscosity, such as the FW and SeS co-digestate, allows a quicker and more sludge flocs or particles transportation from the membrane surface back to the mixed liquor. As a

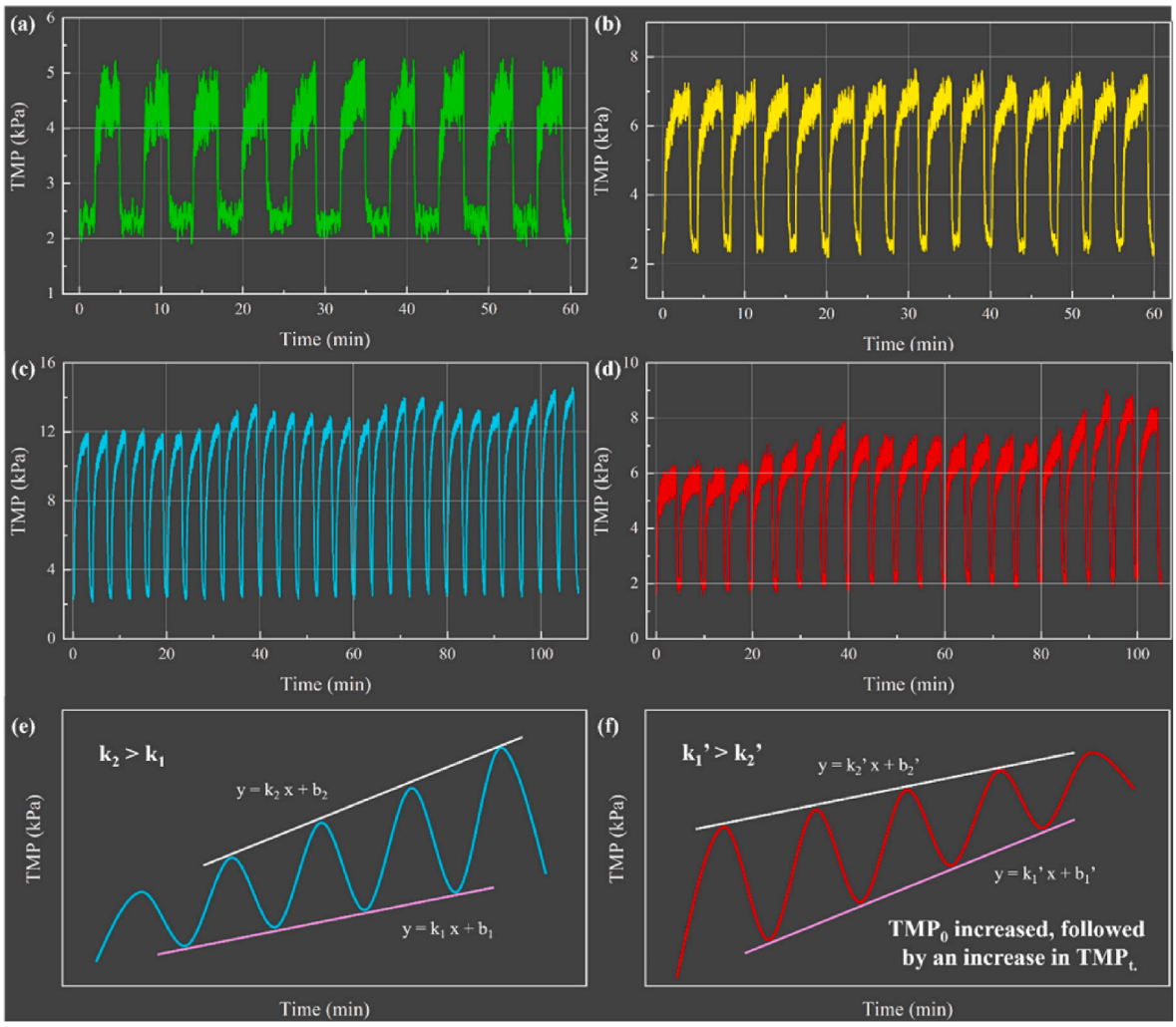

Fig. 6. Real-time TMP curves under different filtration modes: (a) TS = 30 g/L, F/R = 3:3, $J_{inst.}$ = 12 LMH, a low sustainable flux operation in the FW and SeS co-digestion; (b) TS = 30 g/L, F/R = 3:1, $J_{inst.}$ = 12 LMH, the maximum sustainable flux operation in the FW and SeS co-digestion; (c) TS = 30 g/L, F/R = 3:1, $J_{inst.}$ = 15 LMH, an unsustainable flux operation induced by excessive instantaneous flux in the FW and SeS co-digestion; (d) TS = 30 g/L, F/R = 4:1, $J_{inst.}$ = 12 LMH, an unsustainable flux operation induced by inadequate relaxation time in the FW and SeS co-digestion; (e) schematic diagram of a mixed liquid with a high apparent viscosity under an unsustainable process caused by excessive instantaneous flux; (f) schematic diagram of a mixed liquid with a high apparent viscosity under an unsustainable process caused by inadequate relaxation time.

result, TMP_0 can return to the starting values very quickly after relaxation. This is also the reason why TMP_0 kept around the initial value over time in Fig. 6 (c) and (d).

4. Conclusion

In this study, a control strategy of membrane filtration was systematically investigated for the anaerobic co-digestion of FW and SeS at varying TS concentrations to improve sustainable flux and mitigate membrane fouling. The main findings are as follows.

(1) The optimal membrane filtration conditions at the TS concentrations of 30, 25, 20, and 15 g/L were at the instantaneous fluxes of 12, 15, 24, and 24 LMH, and the F/R ratios of 3:1, 5:1, 9:1, and 9:1, respectively. Under these optimized conditions, the maximum sustainable fluxes reached 8.7 ± 0.1, 13.3 ± 0.2, 20.3 ± 0.2, and 20.3 ± 0.6 LMH, which were 4.24, 3.33, 2.18, 2.01, and 1.54 times of those in mono FW digestion.
(2) A TS concentration of 20 g/L is recommended for the FW and SeS co-digestion due to the high sustainable flux and treatment capacity.
(3) The obtained exponential function correlating maximum sustainable flux and TS concentration can be used to forecast the sustainable flux at other TS levels.

CRediT authorship contribution statement

Hui Cheng: Writing – review & editing, Writing – original draft, Investigation, Funding acquisition, Data curation, Conceptualization. **Kaiyi Gu:** Writing – review & editing, Investigation. **Yemei Li:** Investigation. **Guangze Guo:** Investigation. **Chang-Tang Chang:** Writing – review & editing, Data curation. **Wenshan Guo:** Writing – review & editing, Data curation. **Yu-You Li:** Writing – review & editing, Supervision, Conceptualization.

Declaration of competing interest

The authors declare that they have no known competing financial interests or personal relationships that could have appeared to influence the work reported in this paper.

Acknowledgment

This research was funded by the Program for Young Eastern Scholar at Shanghai Institutions of High Education (QD2020014) and Japan Society for the Promotion of Science (JSPS, File No. 18J11537).

Appendix A. Supplementary data

Supplementary data to this article can be found online at https://doi.org/10.1016/j.jenvman.2025.126652.

Data availability

Data will be made available on request.

References

Aslam, A., Khan, S.J., Shahzad, H.M.A., 2022. Anaerobic membrane bioreactors (AnMBRs) for municipal wastewater treatment- potential benefits, constraints, and future perspectives: an updated review. Sci. Total Environ. 802, 149612. https://doi.org/10.1016/j.scitotenv.2021.149612.

Cao, X., Jia, M., Tian, Y., 2023. Rheological properties and dewaterability of anaerobic co-digestion with sewage sludge and food waste: effect of thermal hydrolysis pretreatment and mixing ratios. Water Sci. Technol. 87 (10), 2441–2456. https://doi.org/10.2166/wst.2023.140.

Cheng, H., Hiro, Y., Hojo, T., Li, Y.-Y., 2018. Upgrading methane fermentation of food waste by using a hollow fiber type anaerobic membrane bioreactor. Bioresour. Technol. 267, 386–394. https://doi.org/10.1016/j.biortech.2018.07.045.

Cheng, H., Li, Y., Guo, G., Zhang, T., Qin, Y., Hao, T., Li, Y.-Y., 2020a. Advanced methanogenic performance and fouling mechanism investigation of a high-solid anaerobic membrane bioreactor (AnMBR) for the co-digestion of food waste and sewage sludge. Water Res. 187, 116436. https://doi.org/10.1016/j.watres.2020.116436.

Cheng, H., Li, Y., Hu, Y., Guo, G., Cong, M., Xiao, B., Li, Y.-Y., 2021. Bioenergy recovery from methanogenic co-digestion of food waste and sewage sludge by a high-solid anaerobic membrane bioreactor (AnMBR): mass balance and energy potential. Bioresour. Technol. 326, 124754. https://doi.org/10.1016/j.biortech.2021.124754.

Cheng, H., Li, Y., Kato, H., Li, Y.-Y., 2020b. Enhancement of sustainable flux by optimizing filtration mode of a high-solid anaerobic membrane bioreactor during long-term continuous treatment of food waste. Water Res. 168, 115195. https://doi.org/10.1016/j.watres.2019.115195.

Cheng, H., Qin, H., Li, Y., Guo, G., Liu, J., Li, Y.-Y., 2024. Comparative study of high-performance mesophilic and thermophilic anaerobic membrane bioreactors in the co-digestion of sewage sludge and food waste: methanogenic performance and energy recovery potential. Sci. Total Environ. 912, 169518. https://doi.org/10.1016/j.scitotenv.2023.169518.

Deng, S., Wang, C., Ngo, H.H., Guo, W., You, N., Tang, H., Yu, H., Tang, L., Han, J., 2023. Comparative review on microbial electrochemical technologies for resource recovery from wastewater towards circular economy and carbon neutrality. Bioresour. Technol. 376, 128906. https://doi.org/10.1016/j.biortech.2023.128906.

Fan, J., Chen, Z., Cheng, Y., Ji, H., Hu, C., Qu, J., 2024. Mechanisms and enhancement of hydrogen evolution for membrane anti-fouling and methane upgrading by sacrificed anode in a novel Electro-AnMBR. Water Res., 122881 https://doi.org/10.1016/j.watres.2024.122881.

Field, R.W., Pearce, G.K., 2011. Critical, sustainable and threshold fluxes for membrane filtration with water industry applications. Adv. Colloid Interface Sci. 164 (1), 38–44. https://doi.org/10.1016/j.cis.2010.12.008.

Field, R.W., Wu, D., Howell, J.A., Gupta, B.B., 1995. Critical flux concept for microfiltration fouling. J. Membr. Sci. 100 (3), 259–272. https://doi.org/10.1016/0376-7388(94)00265-Z.

Guo, G., Li, Y., Zhou, S., Chen, Y., Urasaki, K., Qin, Y., Kubota, K., Li, Y.-Y., 2022. Long term operation performance and membrane fouling mechanisms of anaerobic membrane bioreactor treating waste activated sludge at high solid concentration and high flux. Sci. Total Environ. 846, 157435. https://doi.org/10.1016/j.scitotenv.2022.157435.

Guo, G., Zhou, S., Chen, Y., Qin, Y., Huang, X., Li, Y.-Y., 2024. Enhanced methanogenic degradation and membrane fouling associated with protein-EPS by extending sludge retention time in a high-solid anaerobic membrane bioreactor treating concentrated organic sludge. Water Res. 248, 120879. https://doi.org/10.1016/j.watres.2023.120879.

Guo, Y., Luo, Z., Rong, C., Wang, T., Qin, Y., Hanaoka, T., Sakemi, S., Ito, M., Kobayashi, S., Kobayashi, M., Li, Y.-Y., 2022b. The first pilot-scale demonstration of the partial nitritation/anammox-hydroxyapatite process to treat the effluent of the anaerobic membrane bioreactor fed with the actual municipal wastewater. Sci. Total Environ. 807, 151063. https://doi.org/10.1016/j.scitotenv.2021.151063.

Hu, Y., Cai, X., Du, R., Yang, Y., Rong, C., Qin, Y., Li, Y.-Y., 2022. A review on anaerobic membrane bioreactors for enhanced valorization of urban organic wastes: achievements, limitations, energy balance and future perspectives. Sci. Total Environ. 820, 153284. https://doi.org/10.1016/j.scitotenv.2022.153284.

Hu, Y., Du, R., Nitta, S., Ji, J., Rong, C., Cai, X., Qin, Y., Li, Y.-Y., 2021. Identification of sustainable filtration mode of an anaerobic membrane bioreactor for wastewater treatment towards low-fouling operation and efficient bioenergy production. J. Clean. Prod. 329, 129686. https://doi.org/10.1016/j.jclepro.2021.129686.

Hung, P.T., Thuan, T.H., Van Tuyen, N., Quang, C.X., Vigile, M.F., Cassano, A., Galiano, F., Figoli, A., Le Luu, T., 2024. Review about modifications of antifouling polymer membranes in anaerobic membrane bioreactors (AnMBRs) wastewater treatment. Desalination Water Treat. 320, 100873. https://doi.org/10.1016/j.dwt.2024.100873.

Ji, J., Chen, Y., Hu, Y., Ohtsu, A., Ni, J., Li, Y., Sakuma, S., Hojo, T., Chen, R., Li, Y.-Y., 2021. One-year operation of a 20-L submerged anaerobic membrane bioreactor for real domestic wastewater treatment at room temperature: pursuing the optimal HRT and sustainable flux. Sci. Total Environ. 775, 145799. https://doi.org/10.1016/j.scitotenv.2021.145799.

Jiang, M., Huang, J., Li, P., Ataa, B., Gu, J., Wu, Z., Qiao, W., 2023. Optimization of membrane filtration and cleaning strategy in a high solid thermophilic AnMBR treating food waste. Chemosphere 342, 140151. https://doi.org/10.1016/j.chemosphere.2023.140151.

Jiang, M., Qiao, W., Jiang, P., Wu, Z., Lin, M., Sun, Y., Dong, R., 2022. Mitigating membrane fouling in a high solid food waste thermophilic anaerobic membrane bioreactor by incorporating fixed bed bio-carriers. Chemosphere 292, 133488. https://doi.org/10.1016/j.chemosphere.2021.133488.

Jiao, C., You, S., Lei, Z., Zan, F., Li, Q., Li, Y.-Y., Chen, R., 2025. Deciphering biochar-driven membrane fouling mitigation mechanisms in high-solids AnMBRs: a multi-perspective analysis using computational fluid dynamics and interface thermodynamics. Chem. Eng. J. 516, 164161. https://doi.org/10.1016/j.cej.2025.164161.

Kim, J., Bae, E., Park, H., Park, H.-J., Shah, S.S.A., Lee, K., Lee, J., Oh, H.-S., Park, P.-K., Shin, Y.C., Moon, H., Naddeo, V., Choo, K.-H., 2024. Membrane reciprocation and quorum quenching: an innovative combination for fouling control and energy saving in membrane bioreactors. Water Res. 250, 121035. https://doi.org/10.1016/j.watres.2023.121035.

Kong, Z., Hao, T., Chen, H., Xue, Y., Li, D., Pan, Y., Li, Y., Li, Y.-Y., Huang, Y., 2023. Anaerobic membrane bioreactor for carbon-neutral treatment of industrial wastewater containing N, N-dimethylformamide: evaluation of electricity, bio-energy production and carbon emission. Environ. Res. 216, 114615. https://doi.org/10.1016/j.envres.2022.114615.

Kong, Z., Xue, Y., Hao, T., Zhang, Y., Wu, J., Chen, H., Song, L., Rong, C., Li, D., Pan, Y., Li, Y., Li, Y.-Y., 2022. Carbon-neutral treatment of N, N-dimethylformamide-containing industrial wastewater by anaerobic membrane bioreactor (AnMBR): bio-energy recovery and CO_2 emission reduction. Bioresour. Technol. 358, 127396. https://doi.org/10.1016/j.biortech.2022.127396.

Le, T.-S., Nguyen, P.-D., Ngo, H.H., Bui, X.-T., Dang, B.-T., Diels, L., Bui, H.-H., Nguyen, M.-T., Le Quang, D.-T., 2022. Two-stage anaerobic membrane bioreactor for co-treatment of food waste and kitchen wastewater for biogas production and nutrients recovery. Chemosphere 309, 136537. https://doi.org/10.1016/j.chemosphere.2022.136537.

Lei, Z., Ma, Y., Wang, J., Wang, X.C., Li, Q., Chen, R., 2021a. Biochar addition supports high digestion performance and low membrane fouling rate in an anaerobic membrane bioreactor under low temperatures. Bioresour. Technol. 330, 124966. https://doi.org/10.1016/j.biortech.2021.124966.

Lei, Z., Wang, J., Leng, L., Yang, S., Dzakpasu, M., Li, Q., Li, Y.-Y., Wang, X.C., Chen, R., 2021b. New insight into the membrane fouling of anaerobic membrane bioreactors treating sewage: physicochemical and biological characterization of cake and gel layers. J. Membr. Sci. 632, 119383. https://doi.org/10.1016/j.memsci.2021.119383.

Lei, Z., Zheng, J., Liu, J., Li, Q., Xue, J., Yang, Y., Kong, Z., Li, Y.-Y., Chen, R., 2024. Synergic treatment of domestic wastewater and food waste in an anaerobic membrane bioreactor demo plant: process performance, energy consumption, and greenhouse gas emissions. Water Res. 266, 122371. https://doi.org/10.1016/j.watres.2024.122371.

Li, Q., Zhao, W., Cui, S., Gadow, S.I., Qin, Y., Li, Y.-Y., 2024. Synergetic association of hydroxyapatite-mediated biofilm and suspended sludge enhances resilience of partial nitrification/anammox (PN/A) system treating high-strength anaerobic membrane bioreactor (AnMBR) permeate. Bioresour. Technol. 412, 131391. https://doi.org/10.1016/j.biortech.2024.131391.

Li, Y., Ni, J., Cheng, H., Guo, G., Zhang, T., Zhu, A., Qin, Y., Li, Y.-Y., 2023. Enhanced digestion of sludge via co-digestion with food waste in a high-solid anaerobic membrane bioreactor: performance evaluation and microbial response. Sci. Total Environ. 899, 165701. https://doi.org/10.1016/j.scitotenv.2023.165701.

Liu, J., Fu, W., Yu, X., Yang, H., Zhao, D., Wang, Z., Wang, L., Li, X., Tang, C.Y., 2023. Relating critical and limiting fluxes to metastable and long-term stable fluxes in colloidal membrane filtration through collision-attachment theory. Water Res. 238, 120010. https://doi.org/10.1016/j.watres.2023.120010.

Maaz, M., Yasin, M., Aslam, M., Kumar, G., Atabani, A.E., Idrees, M., Anjum, F., Jamil, F., Ahmad, R., Khan, A.L., Lesage, G., Heran, M., Kim, J., 2019. Anaerobic membrane bioreactors for wastewater treatment: novel configurations, fouling control and energy considerations. Bioresour. Technol. 283, 358–372. https://doi.org/10.1016/j.biortech.2019.03.061.

Mahmoud, I., Liao, B., 2017. Effects of sludge concentration and biogas sparging rate on critical flux in a submerged anaerobic membrane bioreactor. J. Water Proc. Eng. 20, 51–60. https://doi.org/10.1016/j.jwpe.2017.09.012.

Min, S., Lee, H., Deng, L., Guo, W., Xu, B., Yong Ng, H., Mehmood, C.T., Zhong, Z., Zamora, R., Khan, E., Ranjan Dash, S., Kim, J., Pishnamazi, M., Park, P.-K., Chae, S. R., 2024. Advanced strategies for mitigation of membrane fouling in anaerobic membrane bioreactors for sustainable wastewater treatment. Chem. Eng. J. 485, 149996. https://doi.org/10.1016/j.cej.2024.149996.

Molaey, R., Appels, L., Yesil, H., Tugtas, A.E., Çalli, B., 2024. Sustainable heavy metal removal from sewage sludge: a review of bioleaching and other emerging technologies. Sci. Total Environ. 955, 177020. https://doi.org/10.1016/j.scitotenv.2024.177020.

Naji, O., Al-juboori, R.A., Khan, A., Yadav, S., Altaee, A., Alpatova, A., Soukane, S., Ghaffour, N., 2021. Ultrasound-assisted membrane technologies for fouling control and performance improvement: a review. J. Water Proc. Eng. 43, 102268. https://doi.org/10.1016/j.jwpe.2021.102268.

Olubukola, A., Gautam, R.K., Kamilya, T., Muthukumaran, S., Navaratna, D., 2022. Development of a dynamic model for effective mitigation of membrane fouling through biogas sparging in submerged anaerobic membrane bioreactors (SAnMBRs). J. Environ. Manag. 323, 116151. https://doi.org/10.1016/j.jenvman.2022.116151.

Osman, R.M., Hodaifa, G., 2023. An overview of anaerobic membrane bioreactors: current developments, fouling problems, and future prospects. J. Environ. Chem. Eng. 11 (6), 111482. https://doi.org/10.1016/j.jece.2023.111482.

Pan, Y., Zhi, Z., Zhen, G., Lu, X., Bakonyi, P., Li, Y.-Y., Zhao, Y., Rajesh Banu, J., 2019. Synergistic effect and biodegradation kinetics of sewage sludge and food waste mesophilic anaerobic co-digestion and the underlying stimulation mechanisms. Fuel 253, 40–49. https://doi.org/10.1016/j.fuel.2019.04.084.

Parihar, R.K., Chaurasia, S.P., Midda, M.O., 2023. An overview of anaerobic membrane bioreactors' evolving research statistics for treating wastewater. Mater. Today Proc. https://doi.org/10.1016/j.matpr.2023.03.156.

Park, C., Kim, H., Hong, S., Choi, S.-I., 2006. Variation and prediction of membrane fouling index under various feed water characteristics. J. Membr. Sci. 284 (1), 248–254. https://doi.org/10.1016/j.memsci.2006.07.036.

Wang, K., Zhang, H., Shen, Y., Li, J., Zhou, W., Song, H., Liu, M., Wang, H., 2023. Impact of salinity on anaerobic ceramic membrane bioreactor for textile wastewater treatment: process performance, membrane fouling and machine learning models. J. Environ. Manag. 345, 118717. https://doi.org/10.1016/j.jenvman.2023.118717.

Wang, M., Liu, Y., Jiang, X., Fang, J., Lyu, Q., Wang, X., Yan, Z., 2021. Multi-omics reveal the structure and function of microbial community in co-digestion of corn straw and pig manure. J. Clean. Prod. 322, 129150. https://doi.org/10.1016/j.jclepro.2021.129150.

Wu, J., Kong, Z., Luo, Z., Qin, Y., Rong, C., Wang, T., Hanaoka, T., Sakemi, S., Ito, M., Kobayashi, S., Kobayashi, M., Xu, K.-Q., Kobayashi, T., Kubota, K., Li, Y.-Y., 2021. A successful start-up of an anaerobic membrane bioreactor (AnMBR) coupled mainstream partial nitritation-anammox (PN/A) system: a pilot-scale study on in-situ NOB elimination, AnAOB growth kinetics, and mainstream treatment performance. Water Res. 207, 117783. https://doi.org/10.1016/j.watres.2021.117783.

Wu, Z., Qiao, W., Li, Y.-Y., Yao, J., Sun, Y., Dong, R., 2023. Chemically and biologically driven carbon transformation flow in MSW leachate treated by a high-solids anaerobic membrane bioreactor system. Chemosphere 335, 139075. https://doi.org/10.1016/j.chemosphere.2023.139075.

Zhang, H., Fu, Z., Guan, D., Zhao, J., Wang, Y., Zhang, Q., Xie, J., Sun, Y., Guo, L., Wang, D., 2023. A comprehensive review on food waste anaerobic co-digestion: current situation and research prospect. Process Saf. Environ. Prot. 179, 546–558. https://doi.org/10.1016/j.psep.2023.09.030.

Zhang, Q., Singh, S., Stuckey, D.C., 2017. Fouling reduction using adsorbents/flocculants in a submerged anaerobic membrane bioreactor. Bioresour. Technol. 239, 226–235. https://doi.org/10.1016/j.biortech.2017.05.022.

Zhang, W., Liang, W., Jin, J., Meng, S., He, Z., Ali, M., Saikaly, P.E., 2024a. Filtration performance of biofilm membrane bioreactor: fouling control by threshold flux operation. Chemosphere 362, 142458. https://doi.org/10.1016/j.chemosphere.2024.142458.

Zhang, X., Fan, Y., Hao, T., Chen, R., Zhang, T., Hu, Y., Li, D., Pan, Y., Li, Y.-Y., Kong, Z., 2024b. Insights into current bio-processes and future perspectives of carbon-neutral treatment of industrial organic wastewater: a critical review. Environ. Res. 241, 117630. https://doi.org/10.1016/j.envres.2023.117630.

Zhou, Z., Tao, Y., Zhang, S., Xiao, Y., Meng, F., Stuckey, D.C., 2019. Size-dependent microbial diversity of sub-visible particles in a submerged anaerobic membrane bioreactor (SAnMBR): implications for membrane fouling. Water Res. 159, 20–29. https://doi.org/10.1016/j.watres.2019.04.050.